Author(s): Suut-Tuule, Elina; Jarg, Tatsiana; Tikker, Priit; Lootus, Ketren-Marlein; Martõnova, Jevgenija; Reitalu, Rauno; Ustrnul, Lukas; Ward, Jas S.; Rjabovs, Vitalijs; Shubin, Kirill; Nallaparaju, Jagadeesh V.; Vendelin, Marko; Preis, Sergei; Öeren, Mario; Rissanen, Kari; Kananovich, Dzmitry; Aav, Riina

Title: Mechanochemically driven covalent self-assembly of a chiral mono-biotinylated hemicucurbit[8]uril

Year: 2024

Version: Published version

Please cite the original version:

Suut-Tuule, E., Jarg, T., Tikker, P., Lootus, K.-M., Martõnova, J., Reitalu, R., Ustrnul, L., Ward, J. S., Rjabovs, V., Shubin, K., Nallaparaju, J. V., Vendelin, M., Preis, S., Öeren, M., Rissanen, K., Kananovich, D., & Aav, R. (2024). Mechanochemically driven covalent self-assembly of a chiral mono-biotinylated hemicucurbit[8]uril. Cell Reports Physical Science, 5(9), Article 102161. https://doi.org/10.1016/j.xcrp.2024.102161

Cell Reports
Physical Science

CellPress
OPEN ACCESS

Article

Mechanochemically driven covalent self-assembly of a chiral mono-biotinylated hemicucurbit[8]uril

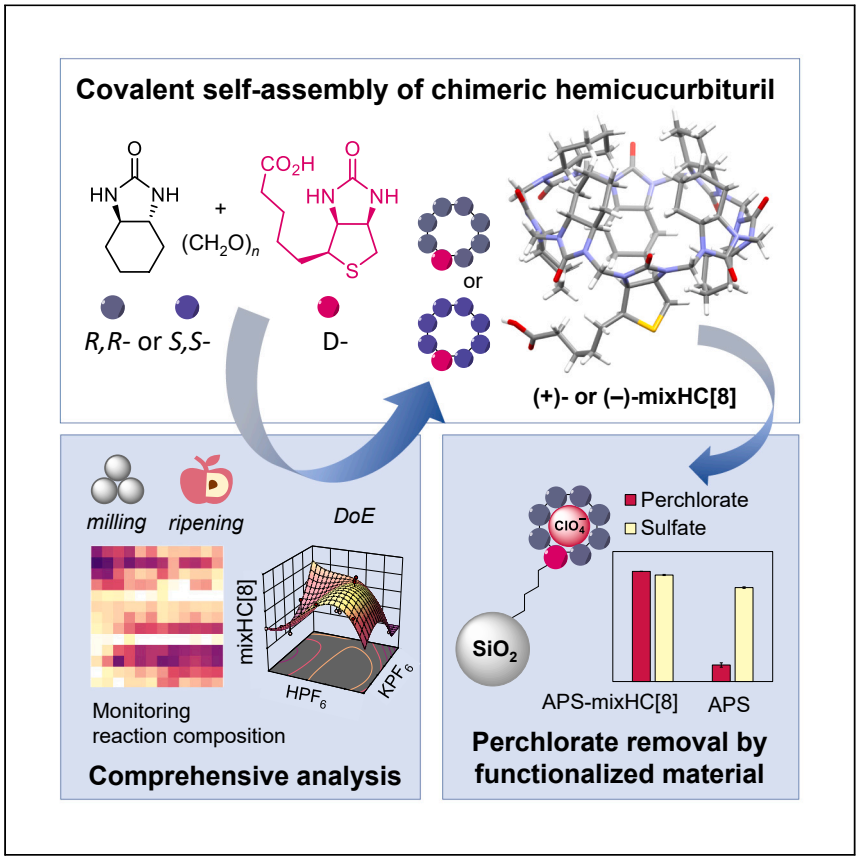

Suut-Tuule and Jarg et al. demonstrate that mechanochemistry enhances reactivity and significantly improves selectivity in the solid-state synthesis of mono-biotinylated hemicucurbit[8]urils. The application of the chimeric macrocycle is showcased by its immobilization on silica and subsequent use as a selective solid-phase extraction material for perchlorate removal.

Elina Suut-Tuule, Tatsiana Jarg, Priit Tikker, ..., Kari Rissanen, Dzmitry Kananovich, Riina Aav

riina.aav@taltech.ee

Highlights

Dynamic covalent chemistry in solid state delivers chimeric hemicucurbit[8]urils

Two major products are amplified from ca. 50,000 possible compounds

Mechanochemistry and anionic templation drive covalent self-assembly

Silica modified by biotinylated macrocycle is suitable for perchlorate capture

Suut-Tuule et al., Cell Reports Physical Science 5, 102161
September 18, 2024
Published by Elsevier Inc.
https://doi.org/10.1016/j.xcrp.2024.102161

Please cite this article in press as: Suut-Tuule et al., Mechanochemically driven covalent self-assembly of a chiral mono-biotinylated hemicucurbit[8]uril, Cell Reports Physical Science (2024), https://doi.org/10.1016/j.xcrp.2024.102161

Cell Reports
Physical Science

Article

Mechanochemically driven covalent self-assembly of a chiral mono-biotinylated hemicucurbit[8]uril

Elina Suut-Tuule,[1,8] Tatsiana Jarg,[1,8] Priit Tikker,[2] Ketren-Marlein Lootus,[1] Jevgenija Martõnova,[1] Rauno Reitalu,[1] Lukas Ustrnul,[1] Jas S. Ward,[3] Vitalijs Rjabovs,[4,5] Kirill Shubin,[6] Jagadeesh V. Nallaparaju,[1] Marko Vendelin,[7] Sergei Preis,[2] Mario Öeren,[1] Kari Rissanen,[3] Dzmitry Kananovich,[1] and Riina Aav[1,9,10,*]

SUMMARY

Solution-based synthesis of complex molecules with high efficiency leverages supramolecular control over covalent bond formation. Herein, we present the mechanosynthesis of chiral mono-biotinylated hemicucurbit[8]urils (mixHC[8]s) via the condensation of D-biotin, (*R,R*)- or (*S,S*)-cyclohexa-1,2-diylurea, and paraformaldehyde. The selectivity of self-assembly is enhanced through mechanochemistry and by fostering non-covalent interactions, achieved by eliminating solvents and conducting the reaction in the solid state. Rigorous analysis of intermediates reveals key processes and chemical parameters influencing dynamic covalent chemistry. The library of ca. 50,000 theoretically predicted intermediates and products leads to covalent self-assembly of chiral hemicucurbiturils. Mechanochemically prepared diastereomeric (−)- and (+)-mixHC[8]s are suitable for anion binding and derivatization. Immobilization of the macrocycles on aminated silica produces a functional material capable of selective capture of anions, as demonstrated by efficient perchlorate removal from a spiked mineral matrix.

INTRODUCTION

The spontaneous organization of molecular species relies on non-covalent interactions, resulting in intricate aggregates. Such supramolecular self-assembly can facilitate the formation of covalent bonds leading to complex molecules and may be exceptionally responsive to minor changes in the reaction conditions, resulting in the amplification of particular products.[1] In the case of increased molecular crowding, the dynamics of an interaction between species is accelerated compared to a dilute environment, which has been demonstrated for strongly hydrogen-bonded base pairs of nucleic acids.[2] Furthermore, in the solid state at extreme concentrations, unobstructed by solvent, the number of non-covalent interactions between counterparts increases, enabling the formation of products that are less favored in solution.[3,4] Mechanochemical activation enhances chemical reactivity and provides a solvent-free sustainable approach in chemical syntheses.[5–7]

Single-bridged cucurbituril-type molecular containers, hemicucurbit[*n*]urils (HC[*n*]s) are renowned for their anion-binding properties and typically assembled from urea monomers in a one-pot reaction with dynamic covalent chemistry (DCC).[8–10] Although the size of the macrocycle can be controlled by anion templation,[8,11–15] HC[*n*]s prevalently consist of six units.[12,16,17] Up to date, 8-membered HC[*n*]s have been synthesized exclusively from chiral C_2-symmetric cyclohexa-1,2-diylurea (CU)

[1]Tallinn University of Technology, Department of Chemistry and Biotechnology, 12618 Tallinn, Estonia

[2]Tallinn University of Technology, Department of Materials and Environmental Technology, 19086 Tallinn, Estonia

[3]University of Jyvaskyla, Department of Chemistry, 40014 Jyväskylä, Finland

[4]National Institute of Chemical Physics and Biophysics, 12618 Tallinn, Estonia

[5]Institute of Chemistry and Chemical Technology, Riga Technical University, 1048 Riga, Latvia

[6]Latvian Institute of Organic Synthesis, 1006 Riga, Latvia

[7]Tallinn University of Technology, Department of Cybernetics, 12618 Tallinn, Estonia

[8]These authors contributed equally

[9]X (formerly Twitter): @RiinaAav

[10]Lead contact

*Correspondence: riina.aav@taltech.ee

https://doi.org/10.1016/j.xcrp.2024.102161

monomers, and the corresponding (*R*,*R*)- and (*S*,*S*)-cyclohexanohemicucurbit[8]urils (cycHC[8]s) can be assembled both in solution[18] and the solid state.[17] Their larger cavity expands the range of applications, and the insertion of another functional monomer, such as D-biotin, into the cycHC[8] scaffold can further enhance receptor versatility. Biotin is a naturally occurring and commercially available compound with a carboxylic group suitable for derivatization. Furthermore, it has previously been used in the synthesis of chiral macrocycles.[13] So far, the reported chimeric HC[*n*]s assembled from non-equivalent urea monomers have been limited to 6-membered hybrid HC[*n*]s prepared in solution via multi-step approaches[19,20] and mono-functionalized bambus[6]urils obtained in a one-pot reaction.[21–23] The difficulties in the single-step formation of non-uniformly composed macrocycles arise from a plethora of possible linear and cyclic intermediates. Consequently, arranging a chaotic mixture into a well-organized molecule presents considerable challenges, and the number of combinations increases with the number of monomeric units.

Mechanochemistry has been utilized in the synthesis of several macrocycles,[17,24–30] inducing covalent assembly of uniformly structured monomers. As mechanosynthesis enables overcoming the solubility barriers and promotes reactions between compounds with drastic polarity differences, its potential can be exploited even further. To the best of our knowledge, there have been no reports describing covalent self-assembly of macrocycles from mixtures of various monomers in the solid state. The formation of chiral chimeric HC[*n*]s via DCC in the solid state could pave the way to novel synthetic approaches, unlocking access to versatile applications.

The present work describes a mechanochemically activated solid-state condensation of (*R*,*R*)- or (*S*,*S*)-CU, D-biotin ((*S*,*S*,*R*)-B), and paraformaldehyde and their selective covalent self-assembly into the enantiopure mono-biotinylated HC[8]s (−)-((*S*,*S*,*R*)(*R*,*R*)$_7$)-mixHC[8] or (+)-((*S*,*S*,*R*)(*S*,*S*)$_7$)-mixHC[8], along with homomeric cycHC[8]s. The challenges of assembling a chimeric mono-functionalized 8-membered macrocycle are related to the number of possible combinations of monomeric units and their chemical reactivity. Fine-tuning of the reaction conditions enabled amplification of the two major products, chimeric mixHC[8] and homomeric cycHC[8], among 498 potential 8-membered HC[*n*]s[31] (Figure 1; theoretical number of linear cyclic oligomers in the supplemental experimental procedures; Data S1).

The covalent assembly process is essentially solvent free and has a very low process mass intensity (PMI; the mass of all used reagents per formed product[32]). The most significant chemical and technical factors affecting macrocyclization were identified with response surface methodology (RSM) and thorough analysis of intermediates by high-performance liquid chromatography-mass spectrometry (HPLC-MS) provided mechanistic insight into this complex process. The affinity of mixHC[8] for selected anions and the subtle differences in the binding properties of the two chimeric diastereomers were determined by isothermal titration calorimetry (ITC) and characterized by single-crystal X-ray crystallography (SC-XRD) and modeling studies. Furthermore, a practical example of the selective anion capture by silica-immobilized mixHC[8] was demonstrated in the efficient removal of perchlorate from a spiked mineral matrix.

RESULTS AND DISCUSSION

Covalent assembly of hemicucurbiturils in the solid state

The first attempts to synthesize mono-functionalized mixHC[8] in solution according to the protocol developed for cycHC[8][18] were promising. The condensation of

Please cite this article in press as: Suut-Tuule et al., Mechanochemically driven covalent self-assembly of a chiral mono-biotinylated hemicucurbit [8]uril, Cell Reports Physical Science (2024), https://doi.org/10.1016/j.xcrp.2024.102161

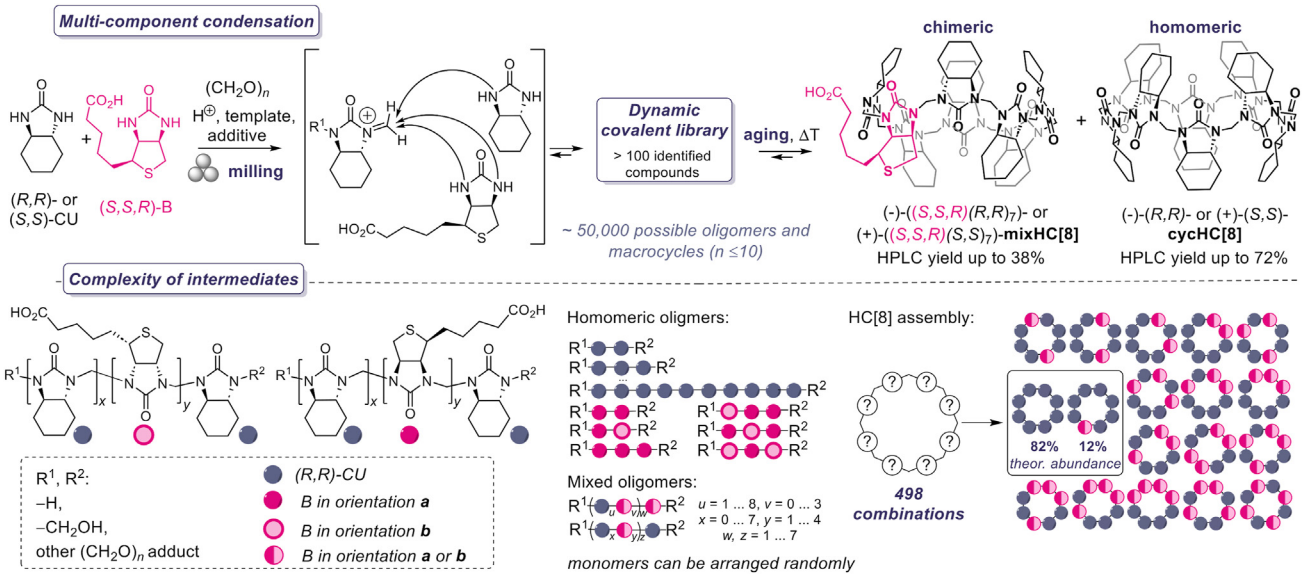

Figure 1. Synthetic scheme and complexity of intermediates during formation of the HC[8]s studied in this work

Multi-component condensation of (*S,S,R*)-biotin (B) and (*R,R*)- or (*S,S*)-cyclohexa-1,2-diylurea (CU) to homomeric cycHC[8]s and chimeric mixHC[8]s. The complexity of the intermediates in the DCL is expressed via possible numbers of oligomers, HC[8]s, and the abundance of major HC[8]s resulting from the 1:7 (B:CU) ratio of starting materials (theoretical number of linear cyclic oligomers in the supplemental experimental procedures; Data S1). The best reaction conditions afford 38% and 34% yields of mixHC[8] and cycHC[8], respectively: 1 equiv B, 7 equiv CU, 8 equiv $(CH_2O)_n$ in the presence of 2 equiv HPF_6 and 1 equiv KPF_6, milled at 30 Hz for 60 min and aged at 60°C for 3 h. (Table S15). The highest yield (72%) of cycHC[8] was observed under the following conditions: 1 equiv B, 15 equiv CU, 16 equiv $(CH_2O)_n$ in the presence of 3 equiv $HClO_4$, milled at 30 Hz for 60 min and aged at 45°C for 24 h (Table S2).

biotin and CU taken in stoichiometric 1:7 molar ratio with paraformaldehyde, mediated by trifluoroacetic acid in acetonitrile, produced mixHC[8] and cycHC[8] in 9% and 38% yields, respectively (see synthesis in solution in the supplemental experimental procedures; Data S1). The ratio of the macrocycles did not reflect the statistical distribution based on the starting monomer ratio, which implied a strong influence of the chemical parameters. In solution-based synthesis, compatibility between the solvent and reagents governs the fast diffusion and mixing of starting materials, intermediates, and products, as well as their reactivity. Poor solubility can obstruct reactions, especially in DCC, due to suppressed exchange between reactants. We envisioned that mixHC[8]s may be assembled with higher efficiency in the solid state, where solubility is not critical, non-covalent interactions are not obstructed by the solvent, and templation is enhanced due to a high concentration of reactants.[3] According to the previous study,[17] covalent self-assembly in the solid state required just a minute amount of a liquid additive[33–35] to facilitate proton transfer and delivery of the anionic template, as well as to promote conformational flexibility. The complexity of the dynamic covalent library (DCL) drastically increases in multi-component reactions; for instance, the incorporation of non-C_2 symmetric (*R,S*)-CU units resulted in higher stereochemical diversity and the formation of several diastereomeric HC[*n*]s (i.e., *cis*-cycHC[6] and inverted-*cis*-cycHC[6]).[36] Similarly, condensation of chiral CU and non-C_2 symmetric biotin into linear and cyclic oligomers can be realized via various combinations, considering the possibility of different orientations of the biotin unit (Figure 1). For instance, all forms with a length of 2 to 10 monomers result in ca. 50,000 cyclic and linear oligomers. However, the number of possible products can be decreased by templation. Variation of position, orientation, and number of B and CU monomers leads to 498 potential 8-membered macrocycles[31] (Figure 1; theoretical number of linear cyclic oligomers in the

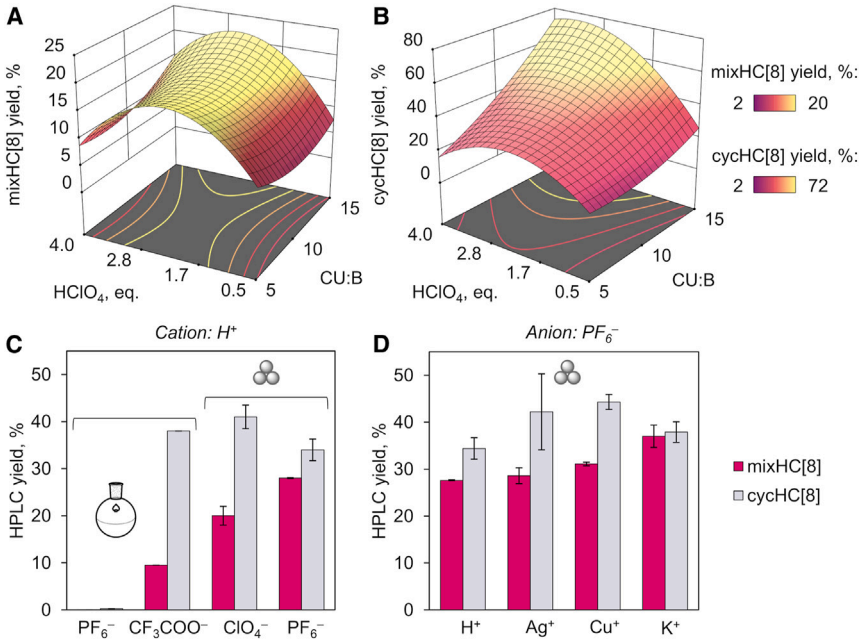

Figure 2. 3D response surfaces and bar charts expressing the formation of HC[8]s

(A and B) 3D response surfaces displaying the influence of the ratio of monomers and loading of aq. $HClO_4$ on the HPLC yields of (A) mixHC[8] and (B) cycHC[8].

(C and D) Bar charts comparing the effect of the acid anions (CF_3COO^-, ClO_4^-, and PF_6^-) in solution and the solid state (C) and hexafluorophosphate salt cations (Ag^+, Cu^+, K^+) in the solid state (D) on the yields of cycHC[8] (gray) and mixHC[8] (magenta). Error bars on HPLC yields express standard deviation between reproduced reactions (n= 2–8). For more details, see Table S7.

supplemental experimental procedures; Data S1). Full conversion of the 1:7 ratio of B and CU into HC[8]s is expected to direct 498 combinations to 12% and 82% of mixHC[8] and cycHC[8], respectively (Figure 1; Table S1).

The fact that solution-phase synthesis did not result in a statistical ratio of more favored HC[8]s encouraged us to study if the selectivity of mono-biotinylated mixHC[8] formation can be increased via tuning the conditions of the mechanosynthesis. To investigate the effect of multiple reaction parameters on the assembly of 8-membered macrocycles, we utilized RSM for experimental design and screening of reaction conditions.[37] The HPLC yields of mixHC[8] and cycHC[8] obtained after the aging step were plotted as 3D response surfaces, highlighting the conditions favorable for the assembly of mixHC[8] compared to cycHC[8] (Figures 2A, 2B, S3, and S4; Tables S2–S6). The ratio of monomers, loading of aqueous mineral acid ($HClO_4$), milling duration, and aging temperature, which affect macrocyclization,[8] were simultaneously explored.

The formation of mixHC[8] and cycHC[8] proved to be sensitive to the monomer ratio and acid loading (Figures 2A and 2B). Variations of the monomer ratios within the range of 1:5 to 1:15 did not significantly affect the yield of chimeric mixHC[8] (Figure 2A; Table S2); however, using an excess of CU clearly resulted in the enhanced generation of cycHC[8] (Figure 2B; Table S2). The quantity of $HClO_4$ appeared to be the vital parameter affecting the formation of mixHC[8]. The highest yields of mixHC[8] were attained within the specific range of $HClO_4$ loadings of 1.2–3.0 equiv (Figure 2A), while cycHC[8] was less dependent on the quantity of acid catalyst. This observation highlights the difference in formation of mixHC[8] and cycHC[8] in

response to varied reaction conditions. The impacts of milling time and aging temperature appeared to be less significant, and the optimal temperature for ripening mixHC[8] was found to range from 40°C to 65°C. RSM helped to reach a 20% yield of mixHC[8] under standard conditions—3 equiv of template, 1 h ball milling followed by 24 h aging at 60°C—selected for further optimization studies.

It was hypothesized that an alternative template could amplify the formation of the target macrocycle. The binding studies for the cycHC[8] receptor revealed the following ranking of anion affinity: SbF_6^- > PF_6^- > ReO_4^- > ClO_4^-.[11] The use of hexafluoroantimonate (SbF_6^-) as a template did not seem practical since $HSbF_6$ mainly exists as the HF/SbF_5 superacid system.[38,39] Hexafluorophosphate (PF_6^-), on the other hand, serves as an efficient template for the synthesis of homomeric cycHC[8] in solution.[18] Due to its advantageous templating potential, HPF_6 was chosen as an alternative reagent to mediate the solid-state synthesis of mixHC[8]. In addition, it is safer to handle than perchlorates, which are known for their undesirable oxidative, flammable, and explosive hazards.[40,41] Interestingly, the use of HPF_6 resulted in decreased formation of homomeric cycHC[8], contrary to an improved yield (28%) of mixHC[8] (Figure 2C; Table S7). Since the mixHC[8] assembly was highly sensitive to the quantity of acid (Figure 2A), we tested three hexafluorophosphate salts ($AgPF_6$, $[Cu(CH_3CN)_4]PF_6$, and KPF_6) as additives to partially substitute the acid while keeping the amount of template anion constant (Figure 2D; Table S7). Additionally, we anticipated that the Ag^+ and Cu^+ cations could serve as potential promoters for the generation of mixHC[8] due to their affinity for biotin.[42–44] As depicted in Figure 2D, the Ag^+ and Cu^+ salts had a negligible effect on the formation of mixHC[8] while improving the yield of homomeric cycHC[8] compared to the reaction with HPF_6. The latter points at the effective decrease in the concentration of antagonistic[45] CU-rich mixed oligomers, which reassembled and provided CU to cyclize into cycHC[8]. The best result was achieved with KPF_6, which afforded the highest yield of mixHC[8] (37%) with the accompanying formation of cycHC[8] (38%) (Figure 2D). Further variation of HPF_6/KPF_6 equivalence by RSM, however, did not improve the formation of mixHC[8] (Tables S8–S12; Figure S8). It was additionally confirmed that the stoichiometric ratio of the starting monomers provided the best mixHC[8] yield (Table S13). Once the key chemical parameters had been identified, the durations of ball milling and aging at moderately elevated temperatures were optimized, leading to the best 38% yield of mixHC[8] in a 4 h total reaction time (Tables S14 and S15; for conditions, see the Figure 1 caption).

The changes in the content of intermediates and products were analyzed by HRMS. Altogether, over 100 reaction species were identified in the crude reaction mixtures during different stages of covalent assembly and mapped based on MS signal intensities (Figures 3A and S9–S13; Tables S16 and S29; MatchMass tool[46]). The results display the dynamic changes in the composition of the reaction mixture during milling and aging. Biotin was found to be incorporated into different linear oligomers $(CU)_x(B)_y$ (x = 1 … 8, y = 1 … 4), as well as into a number of mono-, di-, tri-, and tetra-biotinylated mixHC[*n*]s (n = 6 … 8). Homomeric CU oligomers dominate at the initial phase of the polycondensation reaction (milling time: 5 min) and are kinetically favored products. Consequently, the milling time must be sufficient (60 min; Tables S14 and S15) to enable the accumulation of the slowly generated mixed biotin-containing chains. The content of the mixed oligomers (n = 6–8), which are essential for mixHC[*n*] formation, significantly increased after 45–60 min milling. This difference in the contents of the short- and long-milled mixtures emphasizes the dynamic shuffling of the monomers, which resulted in an increased random distribution of biotin upon prolonged milling. The low content of macrocycles in DCL

CellPress OPEN ACCESS

Cell Reports Physical Science Article

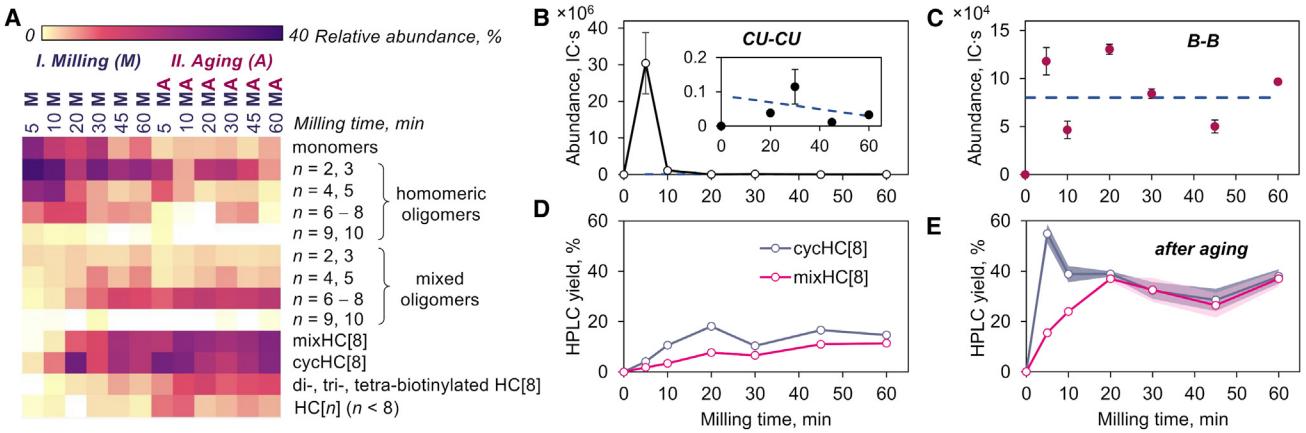

Figure 3. Dynamic covalent library composition and changes in the content of dimers and HC[8]s during mechanosynthesis

DCL composition summarized in a heatmap (A) based on MS abundance of the detected species (Tables S29 and S16; Figure S10); content of homomeric dimers CU-CU (B) and B-B (C) and HPLC yields of macrocycles (D and E) during milling and after aging. The content of the dimers is reported as the MS abundance for triplicate measurements ($n = 3$) ± standard deviation, and the linear fit is expressed as dashed lines. The yields of macrocycles are presented as mean values obtained in a series of replicated experiments ($2 \leq n \leq 4$) with confidence intervals. More details are provided in Figures S11–S15 and Table S19.

directly after milling can be attributed to the unfavorable complexation with the template,[11,17] most likely due to increased entropy during mechanical agitation. The macrocyclic products predominantly ripened at the aging stage, at which point the mixed and homomeric oligomers underwent additional, although less intense, crossover unit exchange. Moreover, crossover between monomers from macrocycles was observed under similar conditions using cycHC[*n*]s and biotin as the starting materials for mixHC[8] synthesis (Table S17), which confirms the dynamic character of the covalent self-assembly.

Further understanding of the dynamic processes and interconversion of intermediates occurring at the milling stage was obtained by tracking the fate of selected short oligomers (Figures 3B and 3C; Table S18). The changes in the content of characteristic dimers and trimers prior to and after the aging stage were determined by HPLC-MS analyses. The collected data confirmed that coupling between the CU monomers is kinetically preferred and occurs at the initial phase of the polycondensation reaction. Thus, the quantity of the CU-CU dimer drastically increased after 5 min of milling and subsequently underwent rapid decay (Figure 3B). Such fast dynamics and decay were absent for the biotin units, reflecting a major difference in the condensation between biotin and CU. In contrast to CU, the condensation of the biotin units to the respective dimer, B-B, reached its maximum at the beginning of the reaction and probably acts as a transient intermediate (Figures 3B and 3C). Similar behavior was observed for the respective trimers (Table S18). The yields of the macrocycles generated at the milling stage did not exceed 20% but greatly increased during aging (Figures 3D and 3E). Notably, the macrocyclic content in the aged mixtures is significantly affected by milling duration, when monomer shuffling occurs. Thus, aging of the short-milled (5 min) reaction mixture, which contained mainly homomeric CU oligomers, resulted in the ripening of cycHC[8] as the dominant product (55% yield), along with a minor quantity of mixHC[8] (16% yield). However, fast reversible C–N bond formation and cleavage during milling caused rapid dynamic changes in the oligomeric profile with a random distribution of the biotin units. Upon prolonged milling (60 min; Tables S14 and S15), the yield of mixHC[8] notably increased from 16% to 37%, with a concurrent decrease in the yield of cycHC[8] to 38%, resulting

Cell Reports
Physical Science
Article

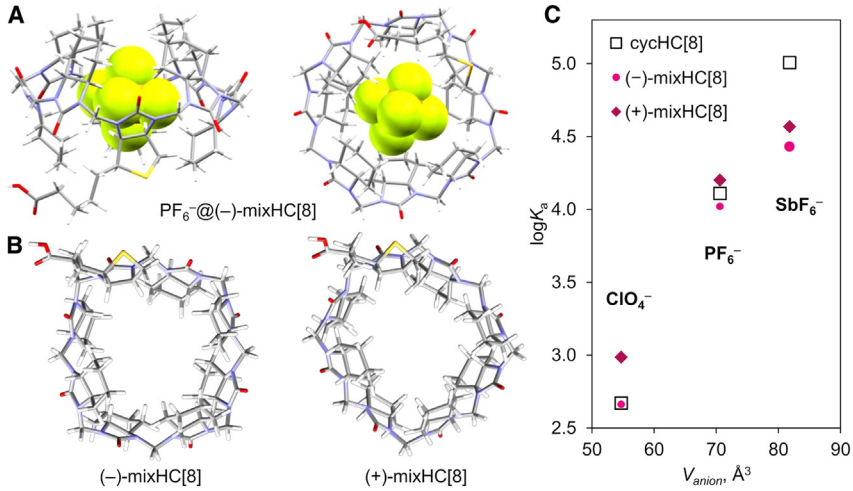

Figure 4. Structures of mixHC[8]s and data on anion binding

PF_6^-@(–)-mixHC[8] inclusion complex from SC-XRD (A) (CCDC: 2251913). DFT low-energy structures of (–)- and (+)-mixHC[8] diastereomers (B) (see the computational study in the supplemental experimental procedures; Data S2). Correlation between anion volumes (V_{anion}) and association constants ($\log K_a$) was determined by ITC for complexes with (TBA)ClO_4, (TBA)PF_6 (TBA = tetrabutylammonium), and $NaSbF_6$ salts in methanol using one-to-one binding model (C) (Table S6.1).

in a 1:1 product ratio. Finally, a close examination of the aging duration (Table S15) revealed that the maximum content of mixHC[8] was achieved in 3 h, when the templated self-assembly process was essentially complete.

The developed mechanochemical procedure significantly surpassed mixHC[8] synthesis in solution, yielding superior selectivity and conversion rates (Table S30). Solution-state processes are affected by diffusion, with diffusion constants varying for monomers, aggregates, and oligomeric intermediates due to size differences. In mechanochemistry, reaction rates do not directly depend on the molecular size of the intermediates but rather on the number of molecular collisions.[47] In addition to the chemical advantages, solvent-free synthesis produces less waste (PMI = 4) compared to the reaction in solution (PMI = 306) and is more sustainable based on the respective green metrics (Table S30).[32]

Diastereoisomeric (–)- and (+)-mixHC[8]s were synthesized via condensation of either (*R*,*R*)-CU or (*S*,*S*)-CU with (*S*,*S*,*R*)-B, isolated in 16% and 11% yields with high purity (88% and 90%, respectively), and characterized by nuclear magnetic resonance (NMR) and infrared spectroscopy (Figures S16–S32).

Anion binding properties

The encapsulation of suitably sized anionic guests by HC[*n*]s is likely governed by electrostatic and orbital interactions.[48] In addition, the anions form weak interactions with C-H groups of HC[*n*]s pointing inside the cavity.[49] Efficient anion recognition has been reported for bambusurils,[22,50–53] heterobambusurils,[54] biotinurils,[55,56] and cycHC[*n*]s.[11] We were fortunate to obtain single crystals of the PF_6^- inclusion complex with (–)-mixHC[8] (Figures 4A and S33–S39; Tables S19 and S20). A DFT modeling study of the mixHC[8] diastereomers (Figure S40; Tables S21–S24; Data S2) revealed clear differences in their conformations (Figure 4B; Data S2). The cavity, which is mainly surrounded by CU units, is mostly

distorted by the biotin position. Therefore, its influence on the anion binding properties was evaluated via comparison of the three HC[8] hosts.

Encapsulation of the selected anions by the mixHC[8]s was studied by ITC (Figures 4C and S51–S54; Table S25); the data for cycHC[8] were available from a previous work.[11] Complexation between the mono-biotinylated macrocycles and chaotropic anions (ClO_4^-, PF_6^-, and SbF_6^-) in methanol and a methanol-water mixture (1:1) occurred as an exothermic enthalpy-driven process. The association constants for PF_6^- were greater than that of ClO_4^- in both media, which explains the better templating properties of PF_6^-. Noticeably, the differences between the affinities of the three HC[8] derivatives are the smallest for the templating PF_6^- anion, while for ClO_4^- and SbF_6^-, either (+)-mixHC[8] or cycHC[8], respectively, exhibit stronger binding. The noted dissimilarities highlight distinctions in the cavities and point to the steric differences of these host compounds, which have potential in a diverse array of applications and unique guest-binding properties.

Selective capture of perchlorate by immobilized mixHC[8]

The mixHC[8] can be utilized to afford functional materials, which was showcased by the selective removal of perchlorates from contaminated soil samples. Perchlorate is a persistent pollutant that adversely affects human health by interfering with thyroid hormone production and occurs in soil, ground water, and food.[40,41] The accumulation of perchlorate in fertilizers, soil, and irrigation water leads to increased plant uptake and subsequent food-chain transfer.[57,58] This pollutant has been found in various environmental matrices and typically originates from human activities.

The carboxylate side chain of mixHC[8] enabled its facile covalent immobilization on the surface of 3-aminopropyl silica gel (APS; Figure 5A).[59] The resulting solid perchlorate-extracting material (mixHC[8]-APS) contained ca. 12% (w/w) of mixHC[8], based on infrared spectroscopic analysis (Figures 5B and S55). Once covalently attached to APS, the macrocycle remains in the solid phase even in the solvents where it is commonly soluble (i.e., dichloromethane, methanol) and can, therefore, be applied in solid-phase extraction. To prove the removal of perchlorate in the presence of other minerals, a regolith simulant[60] was employed as the matrix of the known composition and spiked with $(TBA)ClO_4$, imitating contamination with perchlorate (1% w/w). The obtained model mixture contained cations (Ca^{2+}, Mg^{2+}, Fe^{2+}, Fe^{3+}), oxides, and kosmotropic anions (SO_4^{2-}, CO_3^{2-}) but was essentially free of the organic matter (Table S26). According to ion chromatography analysis (Tables S27 and S28; Figures S56–S59), the methanolic extract of the contaminated matrix contained primarily perchlorate and sulfate, the latter arising from the $MgSO_4$ component (Table S26). Treatment of the methanolic extract with solid mixHC[8]-APS resulted in the complete removal of ClO_4^-, in contrast to non-modified APS, which adsorbed ca. 15% ClO_4^- (Figures 5C and S59; Table S28).

The extraction of sulfate occurred with similar efficiency (ca. 85%–97%) using both APS and mixHC[8]-APS materials, demonstrating that mixHC[8] is not the main contributor responsible for the capture of SO_4^{2-}. The absence of mixHC[8] affinity toward sulfate was additionally confirmed by an ITC experiment (Table S25; Figures S47 and S54).

The captured perchlorate was easily removed by washing mixHC[8]-APS material with water, taking advantage of the weaker binding in the aqueous medium, which demonstrates the potential for the material's reusability.[61]

Cell Reports
Physical Science
Article

CellPress
OPEN ACCESS

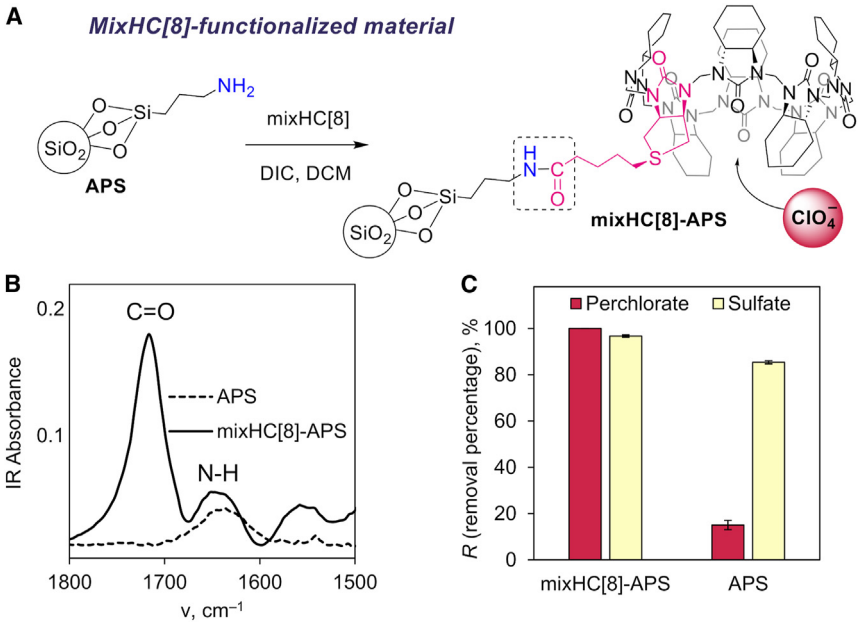

Figure 5. Derivatization of aminated silica by mixHC[8] and perchlorate removal efficiency of the obtained material

Immobilization of mixHC[8] on APS (A), DIC – *N*,*N*′-diisopropylcarbodiimide, and DCM (dichloromethane); characterization of material by infrared (IR) (B) and perchlorate removal from spiked mineral matrix using mixHC[8]-APS and non-modified APS, determined by ion chromatography (C). The error bars represent the standard deviation between the parallel experiments ($n \geq 2$) (isothermal calorimetric titration and immobilization of mixHC[8] on APS in the supplemental experimental procedures).

In conclusion, an efficient mechanochemical protocol for the synthesis of enantiopure mono-biotinylated HC[8]s was developed. The process involves two stages: (1) the mechanochemically assisted and acid-catalyzed polycondensation of D-biotin, (*R*,*R*)- or (*S*,*S*)-CU, and formaldehyde and (2) the aging step, in which the template-driven covalent self-assembly of oligomers into macrocycles takes place. Screening experiments uncovered the key process and chemical parameters affecting the assembly: the ratio of the monomers, the loading of the acid catalyst, and the nature of the templating anion. The present study offers insight into the complex mixture of oligomeric intermediates, including their interconversion and self-organization processes en route to the macrocyclic products. HPLC-MS analysis of short oligomers revealed differences in condensation kinetics of paraformaldehyde with biotin and CU into homomeric dimers and trimers under mechanochemical agitation. The faster condensation of CU led to amplification of the homomeric cycHC[8] during the aging of shortly agitated reaction mixtures. On the contrary, upon prolonged ball milling, which ensures sufficient shuffling of monomers, higher efficiency in the formation of the chimeric mixHC[8] in 38% yield was achieved. The mechanochemically driven solid-state approach allowed for the fine-tuning of the composition of the rich DCL and directing covalent self-assembly processes beyond statistical distribution. Diastereomeric (−)- and (+)-mixHC[8]s were isolated and their structures characterized by DFT, NMR, and SC-XRD methods. Furthermore, the comparison of their affinities toward chaotropic anions pointed at specific binding differences, which makes the chimeric family of HC[8] appealing for host-guest chemistry. The biotin carboxylate group of the mixHC[8] enabled its facile covalent immobilization on aminated silica. The functional material obtained was employed in the selective capture of anions, as

demonstrated by the complete removal of perchlorate from an extract of a mineral model mixture. Further applications of these chiral chimeric hemicucurbiturils are currently being studied.

EXPERIMENTAL PROCEDURES

Resource availability

Lead contact

Further information and requests for resources should be directed to and will be fulfilled by the lead contact, Riina Aav (riina.aav@taltech.ee).

Materials availability

All materials generated in this study are available from the lead contact without restrictions for research purposes.

Data and code availability

All data supporting this study's findings are included in the article and its supplemental information and are also available from the authors upon request. Crystallographic data for the structures reported in this paper have been deposited at the Cambridge Crystallographic Data Center under CCDC: 2251913. Copies of these data can be obtained free of charge via www.ccdc.cam.ac.uk/data_request/cif.

SUPPLEMENTAL INFORMATION

Supplemental information can be found online at https://doi.org/10.1016/j.xcrp.2024.102161.

ACKNOWLEDGMENTS

The authors would like to thank Jasper Adamson and Indrek Reile for input on the NMR analysis. The research by R.A., L.U., D.K., J.S.W., and K.R. was funded by the European Union's H2020- FETOPEN grant 828779 (INITIO). E.S.-T., T.J., K.-M.L., J.V.N., J.M., R.R., and M.O. were financed by Estonian Research Council grants PRG399 and PRG2169. R.A. was funded by the Ministry of Education and Research through Centre of Excellence in Circular Economy for Strategic Mineral and Carbon Resources (01.01.2024–31.12.2030, TK228). The authors also acknowledge COST Action CA18112 "Mechanochemistry for Sustainable Industry" for supporting research in mechanochemistry.

AUTHOR CONTRIBUTIONS

All authors contributed to the manuscript's preparation and have provided their approval for the final version of the manuscript. The authors' specific contributions are as follows: E.S.-T. was the main contributor for the development of the synthesis and mixHC[8] characterization and participated in binding studies; T.J. was the main contributor of the chemical analysis, binding, immobilization, and perchlorate removal studies; P.T. and S.P. contributed to perchlorate removal; K.-M.L., K.S., and J.V.N. contributed to the synthesis; J.M., J.S.W., and K.R. contributed to SC-XRD analysis; R.R. and M.Ö. contributed to computational studies; L.U. contributed to the script for MS data analysis and binding studies; M.V. contributed to the assessment of combinatorics; V.R. contributed to NMR analysis; D.K. contributed to conceptualization of the synthesis, perchlorate removal, and assessment of green metrics; and R.A. contributed to conceptualization of the overall research, data analysis, writing, and supervision.

Cell Reports
Physical Science
Article

CellPress
OPEN ACCESS

DECLARATION OF INTERESTS

This research has been filed for patent application EP23181344.5 and PCT/IB2024/056236. Authors: R.A., E.S.-T., T.J., Tatsiana Nikonovich, D.K., and L.U. Title: "Method of preparation of chimeric HC[n]s, derivatives, and uses thereof," priority date: June 26, 2023.

Received: May 22, 2024
Revised: July 15, 2024
Accepted: July 29, 2024
Published: August 20, 2024

REFERENCES

1. Schnitzer, T., Preuss, M.D., van Basten, J., Schoenmakers, S.M.C., Spiering, A.J.H., Vantomme, G., and Meijer, E.W. (2022). How subtle changes can make a difference: Reproducibility in complex supramolecular systems. Angew. Chem. *61*, e202206738. https://doi.org/10.1002/ange.202206738.

2. Yamaoki, Y., Nagata, T., Kondo, K., Sakamoto, T., Takami, S., and Katahira, M. (2022). Shedding light on the base-pair opening dynamics of nucleic acids in living human cells. Nat. Commun. *13*, 7143. https://doi.org/10.1038/s41467-022-34822-4.

3. Kwon, T.W., Song, B., Nam, K.W., and Stoddart, J.F. (2022). Mechanochemical enhancement of the structural stability of pseudorotaxane intermediates in the synthesis of rotaxanes. J. Am. Chem. Soc. *144*, 12595–12601. https://doi.org/10.1021/jacs.2c00515.

4. Dračínský, M., Hurtado, C.S., Masson, E., and Kaleta, J. (2021). Stuffed pumpkins: Mechanochemical synthesis of host–guest complexes with cucurbit[7]uril. Chem. Commun. *57*, 2132–2135. https://doi.org/10.1039/D1CC00240F.

5. Friščić, T., Mottillo, C., and Titi, H.M. (2020). Mechanochemistry for synthesis. Angew. Chem. *132*, 1030–1041. https://doi.org/10.1002/ange.201906755.

6. Cuccu, F., De Luca, L., Delogu, F., Colacino, E., Solin, N., Mocci, R., and Porcheddu, A. (2022). Mechanochemistry: New tools to navigate the uncharted territory of "impossible" reactions. ChemSusChem *15*, e202200362. https://doi.org/10.1002/cssc.202200362.

7. Reynes, J.F., Isoni, V., and García, F. (2023). Tinkering with mechanochemical tools for scale-up. Angew. Chem., Int. Ed. Engl. *62*, e202300819. https://doi.org/10.1002/anie.202300819.

8. Kaabel, S., and Aav, R. (2018). Templating effects in the dynamic chemistry of cucurbiturils and hemicucurbiturils. Isr. J. Chem. *58*, 296–313. https://doi.org/10.1002/ijch.201700106.

9. Lehn, J.-M. (1999). Dynamic combinatorial chemistry and virtual combinatorial libraries. Chem. Eur J. *5*, 2455–2463. https://doi.org/10.1002/(SICI)1521-3765(19990903)5:9<2455::AID-CHEM2455>3.0.CO;2-H.

10. Corbett, P.T., Leclaire, J., Vial, L., West, K.R., Wietor, J.-L., Sanders, J.K.M., and Otto, S. (2006). Dynamic combinatorial chemistry. Chem. Rev. *106*, 3652–3711. https://doi.org/10.1021/cr020452p.

11. Kaabel, S., Adamson, J., Topić, F., Kiesilä, A., Kalenius, E., Öeren, M., Reimund, M., Prigorchenko, E., Lõokene, A., Reich, H.J., et al. (2017). Chiral hemicucurbit[8]uril as an anion receptor: Selectivity to size, shape and charge distribution. Chem. Sci. *8*, 2184–2190. https://doi.org/10.1039/C6SC05058A.

12. Andersen, N.N., Lisbjerg, M., Eriksen, K., and Pittelkow, M. (2018). Hemicucurbit[n]urils and their derivatives – Synthesis and applications. Isr. J. Chem. *58*, 435–448. https://doi.org/10.1002/ijch.201700129.

13. Lisbjerg, M., Jessen, B.M., Rasmussen, B., Nielsen, B.E., Madsen, A.Ø., and Pittelkow, M. (2014). Discovery of a cyclic 6 + 6 hexamer of D-biotin and formaldehyde. Chem. Sci. *5*, 2647–2650. https://doi.org/10.1039/C4SC00990H.

14. Havel, V., Yawer, M.A., and Sindelar, V. (2015). Real-time analysis of multiple anion mixtures in aqueous media using a single receptor. Chem. Commun. *51*, 4666–4669. https://doi.org/10.1039/C4CC10108A.

15. Yawer, M.A., Havel, V., and Sindelar, V. (2015). A bambusuril macrocycle that binds anions in water with high affinity and selectivity. Angew. Chem., Int. Ed. Engl. *54*, 276–279. https://doi.org/10.1002/anie.201409895.

16. Lizal, T., and Sindelar, V. (2018). Bambusuril anion receptors. Isr. J. Chem. *58*, 326–333. https://doi.org/10.1002/ijch.201700111.

17. Kaabel, S., Stein, R.S., Fomitšenko, M., Järving, I., Friščić, T., and Aav, R. (2019). Size-control by anion templating in mechanochemical synthesis of hemicucurbiturils in the solid state. Angew. Chem., Int. Ed. Engl. *58*, 6230–6234. https://doi.org/10.1002/anie.201813431.

18. Prigorchenko, E., Öeren, M., Kaabel, S., Fomitšenko, M., Reile, I., Järving, I., Tamm, T., Topić, F., Rissanen, K., and Aav, R. (2015). Template-controlled synthesis of chiral cyclohexylhemicucurbit[8]uril. Chem. Commun. *51*, 10921–10924. https://doi.org/10.1039/C5CC04101E.

19. Zeng, Q., Long, Q., Lu, J., Wang, L., You, Y., Yuan, X., Zhang, Q., Ge, Q., Cong, H., and Liu, M. (2021). Synthesis of a novel aminobenzene-containing hemicucurbituril and its fluorescence spectral properties with ions. Beilstein J. Org. Chem. *17*, 2840–2847. https://doi.org/10.3762/bjoc.17.195.

20. Wang, L., Han, J., Pan, R., Yuan, X., You, Y., Cen, X., Zhang, Q., Ge, Q., Cong, H., and Liu, M. (2022). Synthesis of hybrid thiohemicucurbiturils. Tetrahedron Lett. *101*, 153918. https://doi.org/10.1016/j.tetlet.2022.153918.

21. Maršálek, K., and Šindelář, V. (2020). Monofunctionalized bambus[6]urils and their conjugates with crown ethers for liquid–liquid extraction of inorganic salts. Org. Lett. *22*, 1633–1637. https://doi.org/10.1021/acs.orglett.0c00216.

22. De Simone, N.A., Chvojka, M., Lapešová, J., Martínez-Crespo, L., Slávik, P., Sokolov, J., Butler, S.J., Valkenier, H., and Šindelář, V. (2022). Monofunctionalized fluorinated bambusurils and their conjugates for anion transport and extraction. J. Org. Chem. *87*, 9829–9838. https://doi.org/10.1021/acs.joc.2c00870.

23. Del Mauro, A., Lapešová, J., Rando, C., and Šindelář, V. (2024). Merging bambus[6]uril and biotin[6]uril into an enantiomerically pure monofunctionalized hybrid macrocycle. Org. Lett. *26*, 106–109. https://doi.org/10.1021/acs.orglett.3c03715.

24. Langerreiter, D., Kostiainen, M.A., Kaabel, S., and Anaya-Plaza, E. (2022). A greener route to blue: Solid-state synthesis of phthalocyanines. Angew. Chem., Int. Ed. Engl. *61*, e202209033. https://doi.org/10.1002/anie.202209033.

25. Pascu, M., Ruggi, A., Scopelliti, R., and Severin, K. (2013). Synthesis of borasiloxane-based macrocycles by multicomponent condensation reactions in solution or in a ball mill. Chem. Commun. *49*, 45–47. https://doi.org/10.1039/C2CC37538A.

26. Sim, Y., Shi, Y.X., Ganguly, R., Li, Y., and García, F. (2017). Mechanochemical synthesis of phosphazane-based frameworks. Chem. Eur J. *23*, 11279–11285. https://doi.org/10.1002/chem.201701619.

27. Xi, H.-T., Zhao, T., Sun, X.-Q., Miao, C.-B., Zong, T., and Meng, Q. (2013). Rapid and efficient solvent-free synthesis of cyclophanes based on bipyridinium under mechanical ball milling. RSC Adv. *3*, 691–694. https://doi.org/10.1039/C2RA22802E.

28. Kunde, T., Pausch, T., Guńka, P.A., Krzyżanowski, M., Kasprzak, A., and Schmidt,

B.M. (2022). Fast, solvent-free synthesis of ferrocene-containing organic cages via dynamic covalent chemistry in the solid state. Chem. Sci. *13*, 2877–2883. https://doi.org/10.1039/D1SC06372C.

29. Shy, H., Mackin, P., Orvieto, A.S., Gharbharan, D., Peterson, G.R., Bampos, N., and Hamilton, T.D. (2014). The two-step mechanochemical synthesis of porphyrins. Faraday Discuss *170*, 59–69. https://doi.org/10.1039/C3FD00140G.

30. Su, Q., and Hamilton, T.D. (2019). Extending mechanochemical porphyrin synthesis to bulkier aromatics: Tetramesitylporphyrin. Beilstein J. Org. Chem. *15*, 1149–1153. https://doi.org/10.3762/bjoc.15.111.

31. MathWorld–A Wolfram Web Resource. Weisstein, E. W. Necklace. https://mathworld.wolfram.com/Necklace.html.

32. McElroy, C.R., Constantinou, A., Jones, L.C., Summerton, L., and Clark, J.H. (2015). Towards a holistic approach to metrics for the 21st century pharmaceutical industry. Green Chem. *17*, 3111–3121. https://doi.org/10.1039/C5GC00340G.

33. Friščić, T., Childs, S.L., Rizvi, S.A.A., and Jones, W. (2009). The role of solvent in mechanochemical and sonochemical cocrystal formation: A solubility-based approach for predicting cocrystallisation outcome. CrystEngComm *11*, 418–426. https://doi.org/10.1039/B815174A.

34. Do, J.-L., and Friščić, T. (2017). Chemistry 2.0: Developing a new, solvent-free system of chemical synthesis based on mechanochemistry. Synlett *28*, 2066–2092. https://doi.org/10.1055/s-0036-1590854.

35. Belenguer, A.M., Lampronti, G.I., De Mitri, N., Driver, M., Hunter, C.A., and Sanders, J.K.M. (2018). Understanding the influence of surface solvation and structure on polymorph stability: A combined mechanochemical and theoretical approach. J. Am. Chem. Soc. *140*, 17051–17059. https://doi.org/10.1021/jacs.8b08549.

36. Prigorchenko, E., Kaabel, S., Narva, T., Baškir, A., Fomitšenko, M., Adamson, J., Järving, I., Rissanen, K., Tamm, T., and Aav, R. (2019). Formation and trapping of the thermodynamically unfavoured inverted-hemicucurbit[6]uril. Chem. Commun. *55*, 9307–9310. https://doi.org/10.1039/C9CC04990H.

37. Myers, R.H., Montgomery, D.C., and Anderson-Cook, C.M. (2016). Response Surface Methodology: Process and Product Optimization Using Designed Experiments (John Wiley & Sons).

38. Czapla, M., and Skurski, P. (2015). Strength of the Lewis–Brønsted superacids containing In, Sn, and Sb and the electron binding energies of their corresponding superhalogen anions. J. Phys. Chem. A *119*, 12868–12875. https://doi.org/10.1021/acs.jpca.5b10205.

39. Bour, C., Guillot, R., and Gandon, V. (2015). First evidence for the existence of hexafluoroantimonic(V) acid. Chem. Eur J. *21*, 6066–6069. https://doi.org/10.1002/chem.201500334.

40. Urbansky, E.T. (2002). Perchlorate as an environmental contaminant. Environ. Sci. Pollut. Res. Int. *9*, 187–192. https://doi.org/10.1007/BF02987487.

41. Kumarathilaka, P., Oze, C., Indraratne, S.P., and Vithanage, M. (2016). Perchlorate as an emerging contaminant in soil, water and food. Chemosphere *150*, 667–677. https://doi.org/10.1016/j.chemosphere.2016.01.109.

42. Sigel, H., and Scheller, K.H. (1982). Metal ion complexes of D-biotin in solution. Stability of the stereoselective thioether coordination. J. Inorg. Biochem. *16*, 297–310. https://doi.org/10.1016/S0162-0134(00)80266-4.

43. Aoki, K., and Saenger, W. (1983). Interactions of biotin with metal ions. X-ray crystal structure of the polymeric biotin-silver(i) nitrate complex: metal bonding to thioether and ureido carbonyl groups. J. Inorg. Biochem. *19*, 269–273. https://doi.org/10.1016/0162-0134(83)85031-4.

44. Altaf, M., and Stoeckli-Evans, H. (2013). Chiral one- and two-dimensional silver(I)–biotin coordination polymers. Acta Crystallogr. C *69*, 127–137. https://doi.org/10.1107/S0108270113000322.

45. Lehn, J.-M. (2013). Perspectives in chemistry—steps towards complex matter. Angew. Chem., Int. Ed. Engl. *52*, 2836–2850. https://doi.org/10.1002/anie.201208397.

46. Ustrnul, L., Jarg, T., Jantson, M., Osadchuk, I., Anton, L., and Aav, R. (2024). MatchMass: A web-based tool for efficient mass spectrometry data analysis. Preprint at ChemRxiv. https://doi.org/10.26434/chemrxiv-2024-9j8n7.

47. Ma, X., Yuan, W., Bell, S.E.J., and James, S.L. (2014). Better understanding of mechanochemical reactions: Raman monitoring reveals surprisingly simple 'pseudo-fluid' model for a ball milling reaction. Chem. Commun. *50*, 1585–1587. https://doi.org/10.1039/C3CC47898J.

48. Ortolan, A.O., Madureira, L., Rodríguez-Kessler, P.L., Maturana, R.G., Olea Ulloa, C., Caramori, G.F., Parreira, R.L., and Muñoz-Castro, A. (2023). The nature of the central halide encapsulation in bambusuril hosts (BU[6]). Structural and interaction energy insights in BU[6]·X– (X = Cl, Br, I) from relativistic DFT calculations. Inorg. Chim. Acta. *555*, 121596. https://doi.org/10.1016/j.ica.2023.121596.

49. Öeren, M., Shmatova, E., Tamm, T., and Aav, R. (2014). Computational and ion mobility MS study of (All-S)-Cyclohexylhemicucurbit[6]uril structure and complexes. Phys. Chem. Chem. Phys. *16*, 19198–19205. https://doi.org/10.1039/C4CP02202E.

50. Jašíková, L., Rodrigues, M., Lapešová, J., Lízal, T., Šindelář, V., and Roithová, J. (2019). Bambusurils as a mechanistic tool for probing anion effects. Faraday Discuss *220*, 58–70. https://doi.org/10.1039/C9FD00038K.

51. Sokolov, J., Štefek, A., and Šindelář, V. (2020). Functionalized chiral bambusurils: Synthesis and host-guest interactions with chiral carboxylates. ChemPlusChem *85*, 1307–1314. https://doi.org/10.1002/cplu.202000261.

52. Itterheimová, P., Bobacka, J., Šindelář, V., and Lubal, P. (2022). Perchlorate solid-contact ion-selective electrode based on dodecabenzylbambus[6]uril. Chemosensors *10*, 115. https://doi.org/10.3390/chemosensors10030115.

53. Rando, C., Vázquez, J., Sokolov, J., Kokan, Z., Nečas, M., and Šindelář, V. (2022). Highly efficient and selective recognition of dicyanoaurate(I) by a bambusuril macrocycle in water. Angew. Chem., Int. Ed. Engl. *61*, e202210184. https://doi.org/10.1002/anie.202210184.

54. Reany, O., Mohite, A., and Keinan, E. (2018). Hetero-bambusurils. Isr. J. Chem. *58*, 449–460. https://doi.org/10.1002/ijch.201700138.

55. Lisbjerg, M., Nielsen, B.E., Milhøj, B.O., Sauer, S.P.A., and Pittelkow, M. (2015). Anion binding by biotin[6]uril in water. Org. Biomol. Chem. *13*, 369–373. https://doi.org/10.1039/C4OB02211D.

56. Andersen, N.N., Eriksen, K., Lisbjerg, M., Ottesen, M.E., Milhøj, B.O., Sauer, S.P.A., and Pittelkow, M. (2019). Entropy/enthalpy compensation in anion binding: Biotin[6]uril and biotin-l-sulfoxide[6]uril reveal strong solvent dependency. J. Org. Chem. *84*, 2577–2584. https://doi.org/10.1021/acs.joc.8b02797.

57. Calderón, R., Palma, P., Arancibia-Miranda, N., Kim, U.-J., Silva-Moreno, E., and Kannan, K. (2022). Occurrence, distribution and dynamics of perchlorate in soil, water, fertilizers, vegetables and fruits and associated human exposure in Chile. Environ. Geochem. Health *44*, 527–535. https://doi.org/10.1007/s10653-020-00680-6.

58. Chen, Y., Zhu, Z., Wu, X., Zhang, D., Tong, J., Lin, Y., Yin, L., Li, X., Zheng, Q., and Lu, S. (2022). A nationwide investigation of perchlorate levels in staple foods from China: Implications for human exposure and risk assessment. J. Hazard Mater. *439*, 129629. https://doi.org/10.1016/j.jhazmat.2022.129629.

59. Tabakci, M. (2008). Immobilization of calix[6]arene bearing carboxylic acid and amide groups on aminopropyl silica gel and its sorption properties for Cr(VI). J. Inclusion Phenom. Macrocycl. Chem. *61*, 53–60. https://doi.org/10.1007/s10847-007-9392-2.

60. Cannon, K.M., Britt, D.T., Smith, T.M., Fritsche, R.F., and Batcheldor, D. (2019). Mars global simulant MGS-1: A rocknest-based open standard for basaltic Martian regolith simulants. Icarus *317*, 470–478. https://doi.org/10.1016/j.icarus.2018.08.019.

61. Shalima, T., Mishra, K.A., Kaabel, S., Ustrnul, L., Bartkova, S., Tõnsuaadu, K., Heinmaa, I., and Aav, R. (2021). Cyclohexanohemicucurbit[8]uril inclusion complexes with heterocycles and selective extraction of sulfur compounds from water. Front. Chem. *9*, 786746. https://doi.org/10.3389/fchem.2021.786746.